CANDECOMP/PARAFAC (CP) Direction Finding with Multi-Scale Array

Sebastian Miron*, Yang Song†, David Brie*, Kainam Thomas Wong †

*Université de Lorraine, CRAN, UMR 7039, Vandœuvre, F-54506, France, Emails: {sebastian.miron, david.brie}@univ-lorraine.fr
†Hong Kong Polytechnic University, Hong-Kong, Emails: yang.song@connect.polyu.hk; ktwong@ieee.org

Abstract—In this paper, we introduce a novel direction of arrival (DOA) estimation algorithm for an array presenting multiple scales of invariance, based on a CANDECOMP/PARAFAC (CP) model of the data. The proposed approach is a generalization of the results given in [1] to an array presenting an arbitrary number of spatial invariances. We show, on a particular array geometry, that our method could out-perform the ESPRIT-based approach introduced in [2].

I. INTRODUCTION

DOA estimation is a central problem in sensor array processing, with applications in various fields such as radar, sonar or mobile wireless communications. During the last decades numerous methods for DOA estimation have been proposed, ranging from conventional beamforming to high-resolution techniques such as MUSIC [3] or ESPRIT [4]. In [1], Sidiropoulos *et al.* proposed for the first time a direction-finding (DF) approach based on a CP model of the data, and highlighted the link between CP and ESPRIT. Over the next years, several other authors proposed CP-based DF algorithms for *scalar*-sensor or *vector*-sensor arrays (*e.g.* [5]–[8]). The approach proposed in this paper generalizes and extends the philosophy introduced in [1] to arrays presenting multiple scales of invariance. The main idea is to use array configurations decomposable in N-way tensor products, as detailed in the next section. A somewhat similar idea, but in a different context, was also used in [9]. However, the authors of [9] utilize various tensor decompositions of a 2D grid array with two levels of spatial invariances, to illustrate their effect on coherent source estimation performance while, in this paper, we propose an DF algorithm for 3D sensor arrays with an arbitrary number of scales of invariance.

The remainder of this paper is organized as follows: section II presents the proposed multi-scale array configuration and the corresponding data model is derived in section III. In section IV we briefly analyze the identifiability of the proposed data model and an algorithm for DOA parameter estimation is introduced in section V. In section VI, the proposed method is compared in simulations to the ESPRIT-based approach in [2] and some conclusions are drawn in section VII.

II. A MULTI-SCALE ARRAY CONFIGURATION

Consider an array composed of L_1 isotropic identical sensors indexed by $l_1 = 1, \ldots, L_1$. Consider then, L_2 identical

replicas of this array, spatially translated to arbitrary, possibly known locations. The L_2 different copies of the array, indexed by $l_2 = 1, \ldots, L_2$, can now be seen as *subarrays* of a larger (*higher-level*) array. The proposed array structure can be further developed by considering an additional hierarchical level, composed of L_3 translated replicas of the previous array, indexed by $l_3 = 1, \ldots, L_3$. Let us generalize this scheme to a total of N such hierarchical levels, the "highest" level consisting of L_N subarrays indexed by $l_N = 1, \ldots, L_N$. It is worth noting that two different subarrays at a given level n are not necessarily disjoint, *i.e.* they may have in common subarrays/sensors of the previous level $(n-1)$. However, if all subarrays at all levels are disjoint, then the entire array contains a total number of $L = L_1 L_2 \ldots L_N$ identical sensors. Fig. 1 illustrates a three-level array with co-planar sensors.
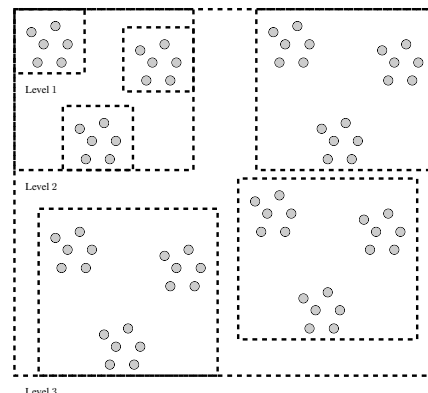

Fig. 1. A multi-scale planar array with three hierarchical levels

Consider also a Cartesian coordinate system $OXYZ$ attached to the considered array. An impinging source is characterized in this coordinate system by its direction cosines u, v, w :

$$\begin{bmatrix} u \\ v \\ w \end{bmatrix} = \begin{bmatrix} \sin\theta\cos\phi \\ \sin\theta\sin\phi \\ \cos\theta \end{bmatrix}, \tag{1}$$

where $\theta \in [0, \pi]$ denotes the source elevation angle measured from the positive Z-axis and $\phi \in [0, 2\pi[$ symbolizes the azimuth angle.

Let us consider a single level-1 subarray of L_1 subarrays. In the coordinate system $OXYZ$, the position of the l_1th sensor of this subarray is given by the vector $(x_{l_1}^{(1)}, y_{l_1}^{(1)}, z_{l_1}^{(1)})$. Consider next L_2 such subarrays. The position of the l_1th sensor

of the l_2th subarray is given by $(x_{l_1}^{(1)} + x_{l_2}^{(2)}, y_{l_1}^{(1)} + y_{l_2}^{(2)}, z_{l_1}^{(1)} + z_{l_2}^{(2)})$, where $(x_{l_2}^{(2)}, y_{l_2}^{(2)}, z_{l_2}^{(2)})$ indicates the spatial displacement of the l_2th subarray compared to the first subarray. It can be easily shown by induction that for a N-level array the position of one sensor is given by $(x_{l_1}^{(1)} + \cdots + x_{l_N}^{(N)}, y_{l_1}^{(1)} + \cdots + y_{l_N}^{(N)}, z_{l_1}^{(1)} + \cdots + z_{l_N}^{(N)})$, where $(x_{l_N}^{(N)}, y_{l_N}^{(N)}, z_{l_N}^{(N)})$ indicates the spatial displacement of the l_Nth subarray compared to the first subarray of the level N (indexed by $l_N = 1$), *etc.*

III. DATA MODEL

Let us symbolize by $a_{l_1, l_2, \ldots, l_N}$ the spatial phase factor of an impinging source at sensor indexed by $l_1, l_2, \ldots, l_N$. Further define $\mathbf{k} = [u \ v \ w]^T$ and $\mathbf{d}_{l_n}^{(n)} = [x_{l_n}^{(n)} \ y_{l_n}^{(n)} \ z_{l_n}^{(n)}]^T$. With the notations introduced above :

$$
\begin{aligned}
a_{l_1, l_2, \ldots, l_N}(\mathbf{k}) &= \exp\left\{ j \frac{2\pi}{\lambda} \sum_{n=1}^{N} \mathbf{k}^T \mathbf{d}_{l_n}^{(n)} \right\} \\
&= \prod_{n=1}^{N} \exp\left\{ j \frac{2\pi}{\lambda} \mathbf{k}^T \mathbf{d}_{l_n}^{(n)} \right\}.
\end{aligned}
\tag{2}
$$

Thus, the array manifold for the entire sensor array is

$$
\mathbf{a}(\mathbf{k}) = \mathbf{a}_1(\mathbf{k}) \otimes \cdots \otimes \mathbf{a}_N(\mathbf{k}),
\tag{3}
$$

with

$$
\mathbf{a}_n(\mathbf{k}) = \begin{bmatrix} e^{j(2\pi/\lambda)\mathbf{k}^T \mathbf{d}_1^{(n)}} \\ \vdots \\ e^{j(2\pi/\lambda)\mathbf{k}^T \mathbf{d}_{L_n}^{(n)}} \end{bmatrix}
\tag{4}
$$

an $L_n \times 1$ vector, $n = 1, \ldots, N$ and " $\otimes$ " the Kronecker product of two matrices.

Consider next, P narrow-band sources with the same center-frequency. The sources are plane-waves, having traveled through a nonconductive homogeneous isotropic medium, impinging upon the array from directions $\mathbf{k}_p = [u_p \ v_p \ w_p]^T$, with $p = 1, \ldots, P$. Denote by $s_p(t)$ the time signal emitted by the pth narrow-band source[1].

Then, the output at time t of the entire sensor array can be expressed as an $L \times 1$ vector

$$
\mathbf{z}(t) = \sum_{p=1}^{P} (\mathbf{a}_1(\mathbf{k}_p) \otimes \cdots \otimes \mathbf{a}_N(\mathbf{k}_p)) s_p(t) + \mathbf{n}(t),
\tag{5}
$$

where $\mathbf{n}(t)$ is a complex-valued zero-mean additive white noise term. Let us assume that we have K temporal observations at time instants $t_1, t_2, \ldots, t_K$. Define the following matrices :

$$
\mathbf{A}_1 = [\mathbf{a}_1(\mathbf{k}_1), \ldots, \mathbf{a}_1(\mathbf{k}_p)]
\tag{6}
$$

$$
\vdots
$$

$$
\mathbf{A}_N = [\mathbf{a}_N(\mathbf{k}_1), \ldots, \mathbf{a}_N(\mathbf{k}_p)]
\tag{7}
$$

---

[1]The incident signals are narrow-band in that their bandwidths are very small compared with the inverse of the wavefronts' transit time across the array.

and

$$
\mathbf{S} = \begin{bmatrix} s_1(t_1) & s_2(t_1) & \ldots & s_p(t_1) \\ s_1(t_2) & s_2(t_2) & \ldots & s_p(t_2) \\ \vdots & \vdots & \ddots & \vdots \\ s_1(t_K) & s_2(t_K) & \ldots & s_p(t_K) \end{bmatrix}.
\tag{8}
$$

The collection of K snapshots of the array can then be organized into an $L \times K$ data matrix as

$$
\mathbf{Z} = [\mathbf{z}(t_1), \ldots, \mathbf{z}(t_K)] = (\mathbf{A}_1 \odot \cdots \odot \mathbf{A}_N)\mathbf{S}^T + \mathbf{N},
\tag{9}
$$

where "$\odot$" denotes the Khatri-Rao (Kronecker column-wise) product of two matrices and $\mathbf{N}$ ($L \times K$) is a complex-valued matrix modeling the sensor noise on the entire array for K snapshots. Equation (9) expresses a $N + 1$ dimensional CP structure of the collected data. In the case where only one snapshot is available, *i.e.* matrix $\mathbf{S}$ is a $1 \times P$ vector, the data model given by (9) becomes

$$
\mathbf{z} = (\mathbf{A}_1 \odot \cdots \odot \mathbf{A}_N)\mathbf{s} + \mathbf{n},
\tag{10}
$$

with $\mathbf{z} = \mathbf{z}(t_1)$, $\mathbf{s} = \mathbf{s}(t_1) = (\mathbf{S}(1, :))^T$ and $\mathbf{n} = \mathbf{N}(:, 1)$. In the definitions above, we used the Matlab notations for columns and rows selection operators. Equation (10) is a vectorized representation of a N dimensional CP data model. It is worth noting that if only one snapshot of the array is available, the $N + 1$ CP model degenerates into a N dimensional model.

IV. MODEL IDENTIFIABILITY

The main advantage of the CP model compared to other source separation approaches is its identifiability under mild conditions. In [10], Kruskal derived a sufficient condition for the identifiability the 3-way CP model. This condition is based on a special notion of matrix rank, called the *Kruskal-rank* or *k-rank*[2] and has been generalized later to N-way arrays by Sidiropoulos and Bro [11]. If applied to the data model given by eq. (9), this condition states that the matrices $\mathbf{A}_1, \ldots, \mathbf{A}_N$ and $\mathbf{S}$ can be uniquely estimated from $\mathbf{Z}$ (up to some trivial indeterminacies) if

$$
\sum_{n=1}^{N} k_{\mathbf{A}_n} + k_{\mathbf{S}} \geq 2P + N,
\tag{11}
$$

where $k_{(.)}$ denotes the Kruskal-rank of a matrix. In the case where the P sources have distinct DOAs and are not fully correlated, the identifiability condition can be reformulated as

$$
\sum_{n=1}^{N} \min(L_n, P) + \min(K, P) \geq 2P + N.
\tag{12}
$$

In general $K > P$, which transforms (12) into $\sum_{n=1}^{N} \min(L_n, P) \geq P + N$. Furthermore, if $L_n > P, n = 1, \ldots, N$, (this could be the case especially for small values of N), than model identifiability is always achieved for $P, N \geq 2$. The brief analysis presented in this section shows that identifiability of the CP model is easily achieved in practical applications. Specific identifiability conditions for the case of fully coherent sources and/or collocated sources can also be derived based, *e.g.* on the partial identifiability results presented in [12]. A more complete identifiability analysis of the presented model will be provided in a future work.

---

[2]The Kruskal-rank of a matrix is the maximum number of independent columns that can selected from that matrix in an arbitrary manner.

V. PARAMETER ESTIMATION

The parameter estimation procedure proposed in the paper can be split into two stages. The first stage consists of the estimation of the N steering vectors $\mathbf{a}_n(\mathbf{k}_p)$ ($n = 1, \ldots, N$) for each of the P sources ($p = 1, \ldots, P$). For that, we exploit the CP structure (9) of the collected data. In the general case of a $N + 1$ order model, an ALS (Alternating Least Squares) procedure can be used to simultaneously estimate the N levels of steering vectors and the temporal sequence of the P sources. In the case of third-order tensors more efficient algorithms than the basic ALS can be used to fit the CP model (see [13]).

The second stage consists of the estimation of the source direction cosines $\mathbf{k}_p$, $p = 1, \ldots, P$ from the steering vectors obtained at the previous stage. Define the following cost functions :

$$\mathcal{J}_n(\mathbf{k}_p) = \|\hat{\mathbf{a}}_n^{(p)} - \mathbf{a}_n(\mathbf{k}_p)\|^2, \qquad (13)$$

with $n = 1, \ldots, N$, and $\hat{\mathbf{a}}_n^{(p)}$ being the nth level estimated steering vector for the pth source. Estimating the DOA parameters for the pth source comes down to minimizing the following criterion:

$$\mathcal{I}_N(\mathbf{k}_p) = \sum_{n=1}^{N} \mathcal{J}_n(\mathbf{k}_p). \qquad (14)$$

This function is non-convex and and highly non-linear; therefore a direct local optimization procedure would fail systematically. In this paper, we propose a sequential strategy for minimizing $\mathcal{I}_N(\mathbf{k}_p)$ based on an iterative refinement of the direction cosines estimates. The method is based on the fact that, in the noise-free case, the N cost-functions in (13) have the same global minimum. We make the assumption that the spatial displacements between sensors inside the level-1 subarrays is such that the maximum distance between adjacent sensors is $\leq \lambda/2$ inside any level-1 subarray, where lambda represents the source wavelength. This assumption is essential to obtaining a set of high-variance but unambiguous direction cosine estimates. On the contrary, the spatial displacement between any two subarrays at the highest level could be $\gg \lambda/2$. This will produce lower variance but cyclically ambiguous estimates of the direction cosines. Under the first assumption, the $\mathcal{J}_1(\mathbf{k}_p)$ function is unimodal inside the definition domain of the DOA parameters. Therefore, any local optimization procedure should converge towards the global minimum of the criterion. Thus, we obtain a set of high-variance, but unambiguous estimates of the DOA parameters, denoted by $\mathbf{k}_{p,1}^*$ with $p = 1, \ldots, P$. These values will then be used, in a second step, as initial point for the minimization of

$$\mathcal{I}_2(\mathbf{k}_p) = \mathcal{J}_1(\mathbf{k}_p) + \mathcal{J}_2(\mathbf{k}_p). \qquad (15)$$

As no assumption is made on the distances between the second level subarrays, $\mathcal{I}_2(\mathbf{k}_p)$ may present more than one local minima. This is why it is crucial to have a good initial point for the optimization procedure. The estimates obtained by the minimization of $\mathcal{I}_2(\mathbf{k}_p)$, denoted by $\mathbf{k}_{p,2}^*$ are then used for the minimization of $\mathcal{I}_3(\mathbf{k}_p) = \sum_{n=1}^{3} \mathcal{J}_n(\mathbf{k}_p)$, and so on until the final estimates are obtained by the minimization of $\mathcal{I}_N(\mathbf{k}_p)$. It is worth noting that as n increases, the number of local minima of the cost function $\mathcal{I}_n$ also increases, and with that, the need for a more and more accurate initial point. This justifies the proposed sequential approach.

The main steps of the algorithm can be summarized as follows:

1) Estimate $\mathbf{A}_1, \ldots, \mathbf{A}_N$ by CP decomposition of the data (see eq. (9) or (10)). The *N-Way toolbox* in [13] could be used to this end.

2) For $p = 1, \ldots, P$ and

for $n = 1, \ldots, N$ compute

$$\mathbf{k}_{p,n}^* = \arg\min_{\mathbf{k}_p} \mathcal{I}_n(\mathbf{k}_p).$$

The minimization of $\mathcal{I}_n$ can be obtained by any local optimization procedure (*e.g.* the Nelder-Mead simplex algorithm), using as initial values the estimates of the previous step $\mathbf{k}_{p,n-1}^*$. Random values, within the parameters definition domain can be used as initialization for the minimization of $\mathcal{I}_1 = \mathcal{J}_1$.

3) Output: the estimated parameters for the P sources: $\hat{\mathbf{k}}_p = (\hat{u}_p, \hat{v}_p, \hat{w}_p) = \mathbf{k}_{p,N}^*$ with $p = 1, \ldots, P$.

VI. SIMULATIONS

In this section, we compare our approach with the one proposed in [2]. A 2-level multi-scale array configuration is considered for simulations. The array consists of a 2×2 square grid at extended spacing and a 5-element half-wavelength spaced cross-shaped subarray at each grid point (*i.e.* $L_1 = 5$ and $L_2 = 4$). In [2], the source' DOAs are estimated using an ESPRIT-based technique. Two types of estimates (coarse but unambiguous, versus fine but cyclically ambiguous) are computed independently for each of the x and y axes of the considered spatial grid, using four matrix pencils altogether. The coarse but unambiguous estimates are then used to disambiguate the fine but cyclically ambiguous DOA estimates. This procedure is followed by a pairing step of the x-axis and y-axis direction cosines of the sources.

The presently considered scenario involves two equal-power narrowband uncorrelated source signals ($P = 2$) impinging respectively from ($\theta_1 = 61.21°, \phi_1 = 73.43°$) and ($\theta_2 = 56.90°, \phi_2 = 23.20°$). A number of $K = 5$ snapshots are simulated in Figure 2(a) and a signal-to-noise ratio of 20 dB is used in Figure 2(b). For each data point, a number of $I = 500$ independent experiments are performed. The additive white noise is complex-value Gaussian distributed. Figures 2(a)-2(b) plot the "composite root-mean-square-error" (CRMSE) of the sources' Cartesian direction-cosine estimates, and their Cramér-Rao Bounds (CRB) versus SNR and versus the number of snapshots, respectively. This "composite root-mean-square-error" (CRMSE) is defined as $\frac{1}{I} \sum_{i=1}^{I} \sqrt{\frac{\delta_{u,p,i}^2 + \delta_{v,p,i}^2}{2}}$, where $\delta_{u,p,i}(\delta_{v,p,i})$ symbolizes the error in estimating the pth source's x-axis (y-axis) direction-cosine during the ith Monte Carlo experiment.

The simulation results show that, for the simulated parameters, our method yields better results than ESPRIT (Fig. 2(a)) for SNR values between 15 dB and 30 dB. This behavior can be explained by the fact that the numbers of parameters estimated by CP equals $(L_1 + L_2 + K)P$ while the number of parameters for ESPRIT is $L_1 L_2 P$. For $K = 5$ snapshots, the number of parameters estimated by CP is inferior to ESPRIT,

which explains the better performance of our approach. As expected, when the noise level is too high or too low, the performances of the two methods are similar. The conclusions of the brief performance analysis presented above are reinforced by Fig. 2(b), where one can observe that CP systematically outperforms ESPRIT for a number of snapshots smaller than $K = 12$. Moreover, the CP method is applied directly on the"raw" data, while ESPRIT requires the estimation of the data covariance matrix for the eigenvalue decomposition. This makes ESPRIT sensitive to the estimation errors of the second order statistics of the data. For the given configuration, both methods can estimate at most 7 sources (see [2] for ESPRIT and section IV for CP). Nevertheless, when the number of sensor increases, ESPRIT can handle more sources than CP, which is the main drawback of our method compared to the one in [2]. The computational burden of CP is also, in general, more important for our method than for ESPRIT. However, powerful algorithms [14], [15] have been developed in the last years that significantly improves the convergence speed of CP decomposition. Moreover, closed-form solutions exist for CP decompositions of Vandermonde structured data [16] (which is often the case in array processing) presenting a computational complexity equivalent to ESPRIT.
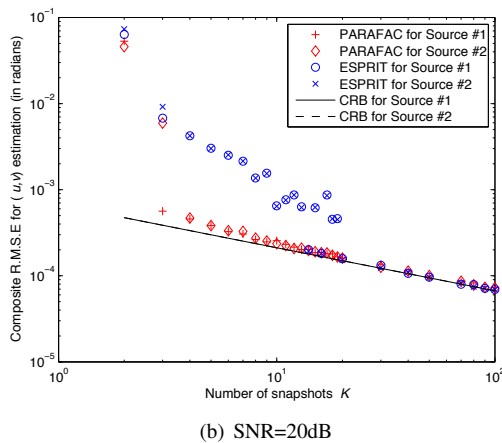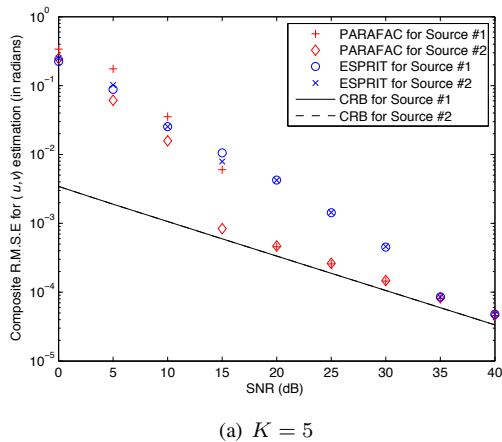
VII. CONCLUSIONS

We introduced in this paper a generalized configuration for a sensor array with multiple scale invariances and derived the corresponding data model. A CP-based algorithm for DOAs estimation with such an array was also proposed, along with a model identifiability analysis. We showed in numerical simulations that, for the particular array geometry given in [2], the proposed method out-performs ESPRIT. The performance of the proposed algorithm will be further evaluated, for various scenarios, in a forthcoming work.

REFERENCES

[1] N. D. Sidiropoulos, R. Bro, and G. B. Giannakis, "Parallel factor analysis in sensor array processing," *IEEE Trans. Signal Process.*, vol. 48, no. 8, pp. 2377–2388, Aug. 2000.

[2] K. T. Wong and M. D. Zoltowski, "Direction-finding with sparse rectangular dual-size spatial invariance arrays," *IEEE Trans. Aerosp. Electron. Syst.*, vol. 34, no. 4, pp. 1320–1336, Oct. 1998.

[3] R. O. Schmidt, *A signal subspace approach to multiple emitter location and spectral estimation*, Ph.D. thesis, Stanford Univ., Stanford, CA, 1981.

[4] R. Roy and T. Kailath, "Esprit-estimation of signal parameters via rotational invariance techniques," *IEEE Trans. Acoust., Speech, Signal Process.*, vol. 37, no. 7, pp. 984 – 995, July 1989.

[5] J. Liang, S. Yang, J. Zhang, L. Gao, and F. Zhao, "4D near-field source localization using cumulant," *EURASIP J. Appl. Signal Process.*, vol. 2007, no. 1, Jan. 2007.

[6] X. Zhang and D. Xu, "Deterministic blind beamforming for electromagnetic vector sensor array," *Progress In Electromagnetics Research*, vol. 84, pp. 363–377, 2008.

[7] D. Nion and N.D. Sidiropoulos, "A parafac-based technique for detection and localization of multiple targets in a MIMO radar system," in *Proc. of IEEE International Conference on Acoustics, Speech and Signal Processing 2009*, Taipei, Apr. 2009, pp. 2077–2080.

[8] X. Guo, S. Miron, D. Brie, S. Zhu, and X. Liao, "A CANDE-COMP/PARAFAC perspective on uniqueness of DOA estimation using a vector sensor array," *IEEE Trans. Signal Process.*, vol. 59, no. 7, pp. 3475–3481, July 2011.

[9] L.-H. Lim and P. Comon, "Blind multilinear identification," *http://arxiv.org/pdf/1212.6663v2*, 2013.

[10] J. B. Kruskal, "Three-way arrays: Rank and uniqueness of trilinear decompositions, with application to arithmetic complexity and statistics," *Linear Algebra Applicat.*, vol. 18, no. 2, pp. 95–138, 1977.

[11] N. D. Sidiropoulos and R. Bro, "On the uniqueness of multilinear decomposition of N-way arrays," *J. Chemometr.*, vol. 14, no. 3, pp. 229–239, 2000.

[12] X. Guo, S. Miron, D. Brie, and A. Stegeman, "Uni-mode and partial uniqueness conditions for CANDECOMP/PARAFAC of three-way arrays with linearly dependent loadings," *SIAM J. Matrix Anal. Appl.*, vol. 33, no. 1, pp. 111–129, 2012.

[13] C. A. Andersson and R. Bro, "The N-way toolbox for MATLAB," *Chemometrics and Intelligent Laboratory Systems*, vol. 52, pp. 1–4, 2000.

[14] R. Bro, N. D. Sidiropoulos, and G. B. Giannakis, "A fast least squares algorithm for separating trilinear mixtures," in *Proc. Int. Workshop Independent Component Analysis and Blind Signal Separation (ICA'99)*, Aussois, France, Jan. 1999.

[15] G. Tomasi and R. Bro, "A comparison of algorithms for fitting the PARAFAC model," *Computational Statistics & Data Analysis*, vol. 50, pp. 1700–1734, 2006.

[16] M. Sorensen and L. De Lathauwer, "Tensor decompositions with Vandermonde factor and applications in signal processing," in *Proc. of the Asilomar Conference on Signals, Systems and Computers*, California, USA, Nov. 2012.

(a) $K = 5$

(b) SNR=20dB

Fig. 2. The composite mean-square-error of the Cartesian direction-cosines estimates.